Dawn Gamma Ray and Neutron Detector DC034 Activity Report

NASA Dawn Mission document, Version 1.2, 4-Feb-2010

Thomas H. Prettyman

Planetary Science Institute

Activities Completed

Name	Description	RSOE file(s)[1]
DC003	Initial Checkout [2,4]	dc003a.03.rsoe.pdf
DC014	Earth-Mars Cruise [2,4]	dc014b_payload.02.rsoe.pdf
DC022	Earth-Mars Cruise [3,4]	dc022a.00.rsoe.pdf
DC023	Mars Gravity Assist [3,4]	dc023b.00.rsoe.pdf dc023c.00.rsoe.pdf (safe mode recovery)
DC024	Mars-Vesta Cruise [4]	dc024a.01.rsoe.pdf
DC034	**Mars-Vesta Cruise**	**dc034b.00.rsoe.pdf**

Summary

GRaND was operated during DC034 (Mars-Vesta Cruise) from 30-Nov-2009 to 7-Dec-2009. Objectives of the activity included:

- Acquisition of background counting data;
- Semi-annual assessment of instrument state of health;
- Optimization of instrument settings;
    - Determine the $^{10}B(n,\alpha)$ reaction peak centroid as a function of high voltage for the –Z phoswich;
    - Determine optimal coincidence window settings for CAT2 (coincidence between the $^{10}B(n,\alpha)^{7}Li^*$ reaction peak in boron-loaded plastic (BLP) and full energy deposition of the associated 478 keV gamma ray ($^{7}Li^* \rightarrow {}^{7}Li + \gamma_{478}$);

As in all previous activities, counting data were acquired for quiet Sun conditions. In addition, for the first time, GRaND was operated concurrently with the Ion Propulsion System (IPS). Key issues and events:

- GRaND functioned nominally; Data were processed to Level1a and delivered to DSC;
- Continued reduction in the resolution of the CZT sensors due to radiation damage was observed; annealing needs to be included in planning activities for Vesta approach;
- Adjustments in CAT2 parameters verified assumptions regarding instrument function;
- IPS operations have a minor influence on GRaND, possibly due to spacecraft charging;
- Operational procedures improved with lessons learned on timing of commands/telemetry.

Data

Level0 data were processed by the Level1a pipeline [3] and were delivered to the Dawn Science Center (DSC) for distribution to the project and science team on 12-Dec-2009.

Table 1. Level0 data summary. The number of science records (NSR) processed and the number of instances of SCLK regression (SCR) of science data packets is provided.

Level 0 PB directory	**Science UTC Begin/End**	**NSR/SCR**	**Instrument state**
09334\	2009-11-30T12:11:55 2009-11-30T14:28:50	46/0	Power on and high voltage ramp-up; configure for data acquisition.
09335\	2009-11-30T14:31:25 2009-12-01T07:09:25*	0/0	SOH data only.
09337\	2009-11-30T14:32:20 2009-12-03T12:58:55	1203/0	TELREADOUT=210s TELSOH=35s Parameter variations (Table 2)
09341\	2009-12-03T13:05:45 2009-12-07T07:58:45	1557/0	TELREADOUT=210s TELSOH=35s Parameter variations (Table 2), HV ramp-down and power off.

*First and last time-stamps from the SOH data.

Table 2. Summary of parameter variations. Only instrument settings that changed are listed. The data are from the DC034 state files. The column labels are defined in the STATE FMT file.

Start Time (UTC-SCET)	-Z phoswich HV (V)	L_BGO_CW	H_BGO_CW	L_BGO_ROI	H_BGO_ROI	L_BLP_MY_CW	H_BLP_MY_CW
2009-12-01T07:10:25	1058.82	27	52	15	78	5	50
2009-12-02T13:02:25	1058.82	1	64	1	64	1	64
2009-12-02T17:01:25	1058.82	1	64	1	64	5	50
2009-12-02T21:01:25	1058.82	9	25	1	64	12	44
2009-12-03T01:00:25	1058.82	12	22	1	64	12	44
2009-12-03T05:00:25	1088.24	12	22	1	64	12	44
2009-12-03T12:06:25	1117.65	12	22	1	64	12	44
2009-12-03T13:02:25	1058.82	12	22	1	64	12	44
	-Z phoswich HV (DN)	L_BLP_PY_CW	H_BLP_PY_CW	L_BLP_MZ_CW	H_BLP_MZ_CW	L_BLP_PZ_CW	H_BLP_PZ_CW
2009-12-01T07:10:25	180	5	50	5	50	5	50
2009-12-02T13:02:25	180	1	64	1	64	1	64
2009-12-02T17:01:25	180	5	50	5	50	5	50
2009-12-02T21:01:25	180	15	40	12	40	5	50
2009-12-03T01:00:25	180	15	40	12	40	5	50
2009-12-03T05:00:25	185	15	40	1	64	5	50
2009-12-03T12:06:25	190	15	40	1	64	5	50
2009-12-03T13:02:25	180	15	40	12	40	5	50

Instrument Optimization: High Voltage

The sensitivity of GRaND to thermal and epithermal neutrons depends on the signal-to-background ratios for theCAT1 (single phoswich interaction) 93 keV peak for the $^{10}B(n,\alpha)$ reaction in the boron-loaded-plastic and the $^{6}Li(n,\alpha)$ reaction in the Li-loaded glass. The peaks are well-separated in pulse height. When the thermal and epithermal neutron flux is low (such as during cruise), the peaks are difficult to discern (e.g., see Fig. 1). Underlying the peaks is a background continuum produced by gamma rays and energetic particles not rejected by anticoincidence. In addition, electronic noise is present at low pulse amplitudes, which strongly influences the precision of the 93 keV peak. By increasing the high voltage applied to the photomultiplier tube, the pulse height of the reaction peaks can be increased well above the noise so that they can be measured with high precision.

In DC034, data were acquired for the spacecraft-pointing (-Z) phoswich for three HV settings, including the nominal 180DN setting used throughout development and cruise. The –Z phoswich was selected because during cruise neutrons originate from the spacecraft and the counting rate for the –Z phoswich is higher than the outboard phoswich. Both phoswiches have similar light output characteristics and are "dimmer" than the L-shaped side scintillators. The objective of the DC034 measurements was to determine whether the sensitivity of the phoswiches could be improved by increasing high voltage to move the 93 keV further above the noise.

Data used to assess the performance of the –Z phoswich are listed in Table 3. CAT1 Spectra for the three HV settings are shown in Fig. 1, which shows that the reaction peaks are near the detection limits. The spectra were analyzed by fitting the spectra with two Gaussians (for the reaction peaks) and a log-log quadratic for the background. The fitted peaks are compared to the background subtracted data in Fig. 2. Peak areas and centroids for the peaks are listed in Table 4.

The analysis shows that the peak centroids increase with HV as expected. The peak counting rates are constant within the quoted uncertainties (to 3σ) as HV changes. For the 93 keV peak, the relative error in the area improves significantly with increasing HV. In contrast, the relative error increases with increasing HV for the Li reaction peak. One explanation for the behavior of the 93 keV peak is that increasing HV moves the peak above the noise into a region of relatively low background. Consequently, an increase in HV would likely be beneficial for measuring the 93 keV peak ; however, the width spanned by the Li reaction peak increases with HV, and at the highest setting, the upper end of the peak is close to the rail. The intermediate HV setting (DN185) would be a reasonable choice for measurements at Vesta. Final selection between the nominal HV (DN180) and the increased HV (DN185) will be made based on data acquired early in LAMO.

Table 3. Summary of data summed to produce the spectra in Fig. 1.

High voltage setting	Number of science data records, TELREADOUT (s)	Directory and state (name of the directory & the instrument state index from the .STA file)
1059V , 180DN	68, 210s	input_directory='MVC\09337\' & state=8
1088V, 185DN	68, 210s	input_directory='MVC\09337\' & state=11
1118V, 190DN	52, 210s	input_directory='MVC\09337\' & state=14

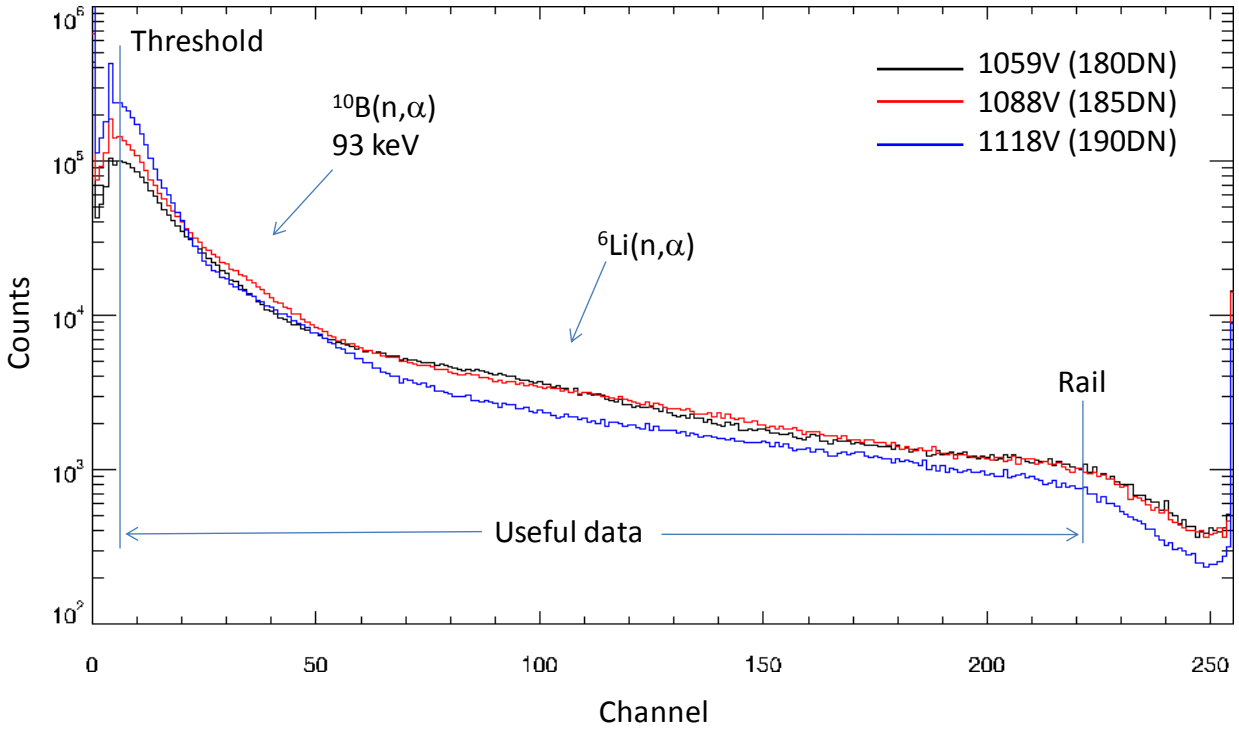

Figure 1. CAT1 pulse height spectrum (single interaction with the –Z phoswich) for three high voltage settings. DN180 (1059V) was used as the nominal setting during development and cruise. Approximate locations of the peaks from neutron reactions with ^{10}B and ^{6}Li are indicated; however, the background continuum due to gamma ray interactions and noise is so large that the peaks are difficult to see. The approximate positions of the low energy electronic threshold and high energy rail are shown.

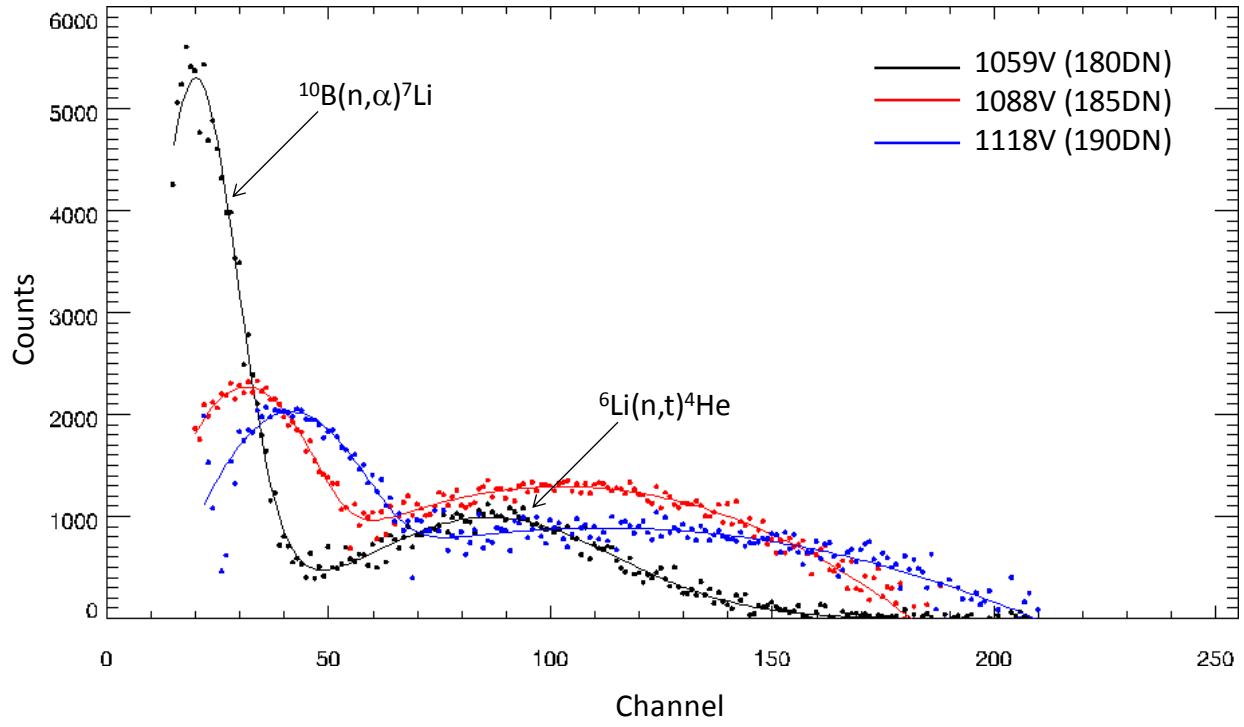

Figure 2. Results of least squares fits of the spectra in Fig. 1 to two Gaussians and a background function. The background (not shown) was modeled as a log-log quadratic. The fitted "double peaks" are compared to the background-subtracted data. For each spectrum, the lower peak is the ^{10}B(n,α) peak. The upper peak is the ^{6}Li(n,α) peak. The centroid and width of both peaks increases with increasing high voltage.

Table 4. Peak areas and centroids from the analysis of spectra shown in Fig. 1. Propagated errors are shown in parentheses.

High voltage setting	^{10}B(n,α) peak Area (counts)	Peak error relative error	^{10}B(n,α) peak centroid (channels)	^{6}Li(n,α) peak Area (counts)	Peak error relative error	^{6}Li(n,α) peak centroid (channels)
1059V , 180DN	126475.61 (20726.592)	16.4%	19.927799 (1.0951335)	70582.226 (5278.7742)	7.5%	86.413991 (1.3645493)
1088V, 185DN	74832.973 (8559.6754)	11.4%	31.288323 (0.59963554)	71789.867 (8595.1161)	11.9%	102.66567 (2.7906707)
1118V, 190DN	56098.030 (3220.7323)	5.7%	41.245928 (0.36390550)	57564.790 (13095.359)	22.7%	112.00000 (0.00000000)*

*The error is zero because the fitted parameter was at the upper bound specified in the analysis.

CZT Array Performance: Radiation Damage

Throughout cruise, the resolution of the CZT has degraded, most likely due to gradual accumulation of radiation damage from galactic cosmic rays.[7] Spectra acquired during ICO and DC034 are compared in Fig. 3. The width of the 511 keV positron annihilation peak has gradually increased such that annealing at high temperature to remove the damage should be considered prior science operations at Vesta. Work is underway to plan a dry run the annealing process in 2010, well in advance of the Vesta encounter.

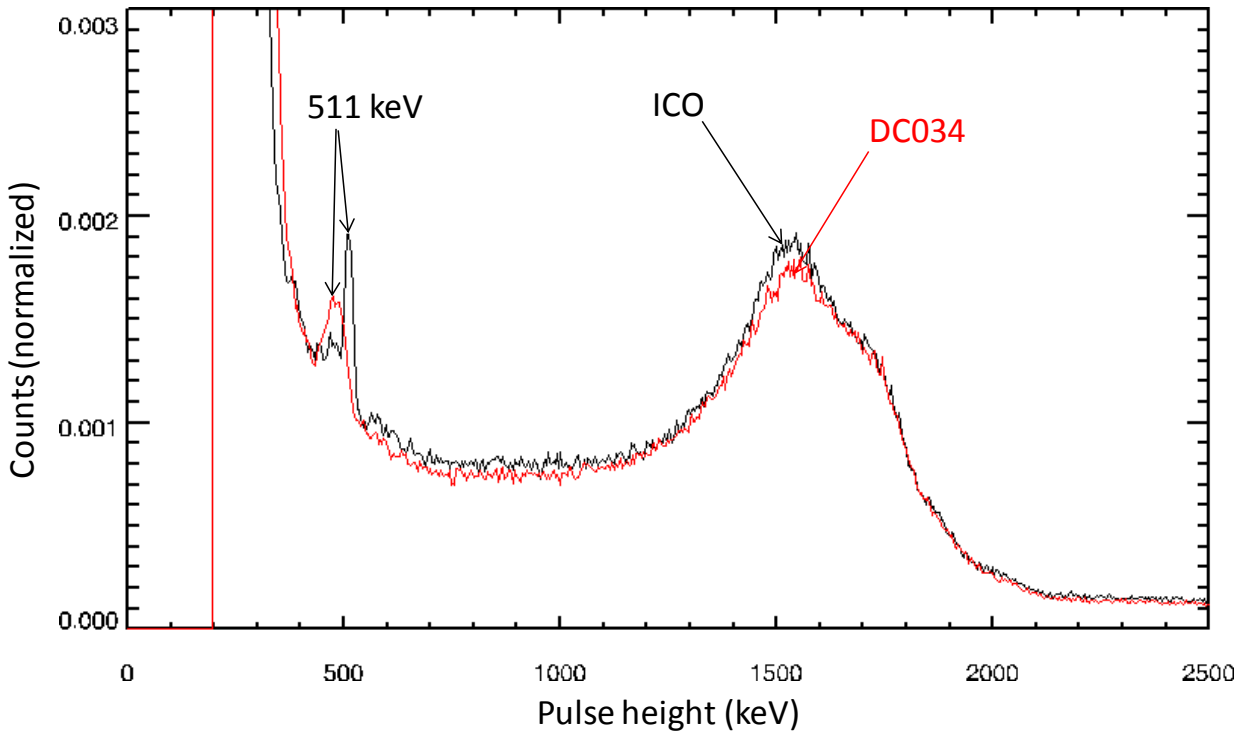

Figure 3. Cumulative pulse height spectra for the CZT array from ICO (input_directory='ICO\07293_grd\' & state=0) and DC034 (input_directory='MVC\09341\' & state=3).

IPS Operations

At about 6:09 (UTC/SCET) on day 339 (2009-12-5), the dead time counter on GRaND began to gradually increase, achieving a steady value about 8 hours later on the same day (Figure 4). The transition corresponds to the commencement of Ion Propulsion System (IPS) operations, which entered diode mode for about an hour followed by continuous operation of thruster 1 [5,6]. We hypothesize that the operation of the neutralizer and ion engine result in charging of the spacecraft, which might change the voltage reference for thresholds in the analog counting circuits on GRaND, resulting in the acceptance of low amplitude pulses (noise). The change is not large enough to affect the analysis of GRaND data in that it would result in less than a 2% error in dead-time-corrected counting rates. So, we conclude that GRaND is insensitive to IPS operations.

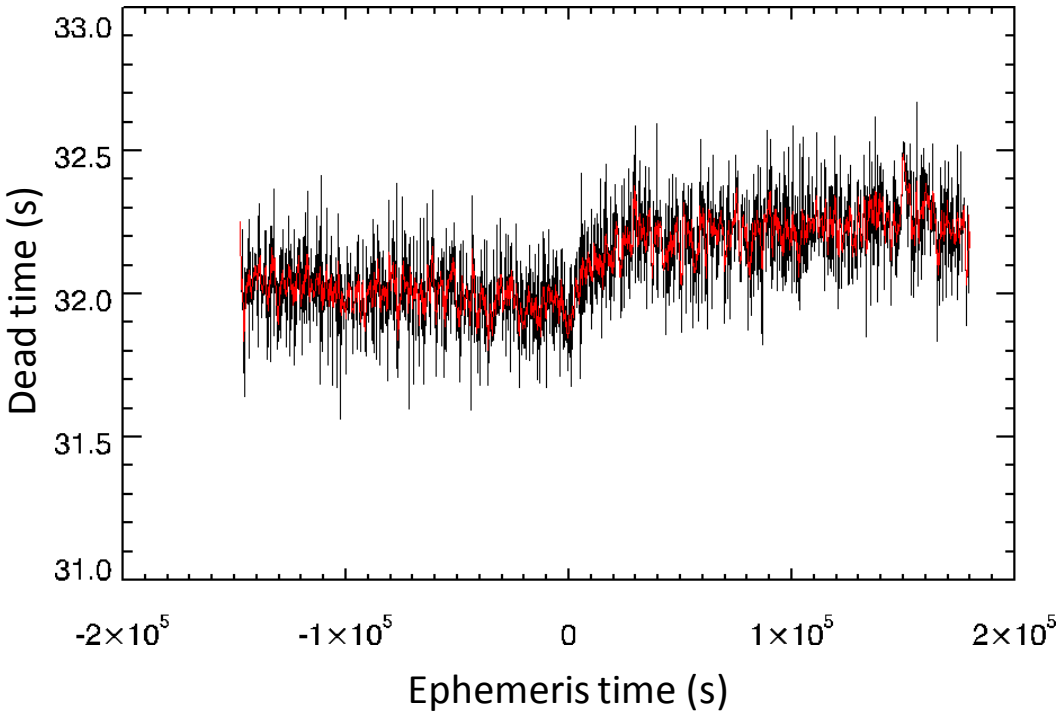

Figure 4. Dead time from the science records plotted against ephemeris time relative to 2009-12-05T06:06:15 (record 701 of Playback-03941), which corresponds roughly t o the start of IPS operations. The data have been corrected for roll-over of the dead time counter (2x roll over was observed during each 210s accumulation interval). The data were smoothed with a 5-point boxcar filter (red) to guide the eye.

CAT2 Parameter Adjustment

For all activities prior to DC034, the BGO CAT2 coincidence windows did not bracket the 478 keV peak, due to the assumption that the window commands referred to the 1024-channel (10 bit) spectrum. It was discovered that the commands for setting the BGO CAT2 coincidence and region of interest windows referred to a 512-channel (9 bit) spectrum, as described in [4]. Based on this information, the CAT2 windows were adjusted in DC034 to bracket the 478 keV peak (Table 2). A key outcome of this DC034 was to revise the startup scripts to use broad (1-64) coincidence and region of interest windows on startup followed by optimization of the window parameters using the Non-Interactive Payload Command (NIPC) process.

References and Notes

1. RSOE files provide a time-ordered list of spacecraft and payload events. They are for internal project use only because they contain information subject to export control.
2. Prettyman, T.H. (2008), GRaND Operations During Cruise: DC003 and DC014, Version 1.3, 26-Sep-2008, NASA Dawn mission document.
3. Prettyman, T.H. (2009), Dawn Mission Mars Gravity Assist: Preliminary Report for GRaND, v1.1, 3-Mar-2009, NASA Dawn mission document.
4. Prettyman, T.H. and W.C. Feldman (2010), PDS Data Processing: Gamma Ray and Neutron Detector, Version 2.2, 2-Feb-2010, NASA Dawn mission document.
5. Garner, C.E. (2009), private communication, Excel spreadsheet – 'IPS Start_Stop Times_7-Jan-2009.xls'.
6. Brophy, J. R., M. G. Marcucci, G. B. Ganapathi, C. E. Garner, M. D. Henry, B. Nakazono, D. Noon (2003), The ion propulsion system for Dawn, 2003 Joint Propulsion Conference, Huntsville, Alabama, 20-Jul-2003, AIAA publication AIAA-2003-4542.